Det Kongelige Danske Videnskabernes Selskab
Matematisk-fysiske Meddelelser, bind **30**, nr. 13

Dan. Mat. Fys. Medd. **30**, no. 13 (1955)

DEDICATED TO PROFESSOR NIELS BOHR ON THE OCCASION OF HIS 70TH BIRTHDAY

SPECTROSCOPIC INVESTIGATIONS OF SEPARATED KRYPTON ISOTOPES

BY

EBBE RASMUSSEN AND VICTOR MIDDELBOE

København 1955
i kommission hos Ejnar Munksgaard

Printed in Denmark.
Bianco Lunos Bogtrykkeri A-S.

1. Introduction.

The hyperfine structure (hfs) of spectral lines of krypton have previously been examined by various investigators making use of normal krypton containing the isotopes in their natural abundances. The purpose of the earlier investigations was to measure interferometrically with the greatest possible accuracy the wavelengths of certain krypton lines, in an effort to confirm the suggestion that one of them might be more suited to be the primary standard of wavelength than the red line of cadmium. In the course of such investigations C. J. HUMPHREYS[1] in 1931 discovered and measured the hfs of several krypton arc lines, but did not, however, assign the hfs to nuclear properties.

A higher resolving power was obtained in 1933 by H. KOPFERMANN and N. WIETH-KNUDSEN[2], who succeeded in analysing the hfs of some partially resolved lines amongst the group of strong lines in the infra-red. The greater part of the total intensity of each of these lines was concentrated in the central component and this was described as being due to the even isotopes ($Z = 78$, 80, 82, 84, and 86), which compose altogether 88.5 % of natural krypton, whereas the odd isotope ($Z = 83$), composing the remaining 11,5 %, was held responsible for the faint satellites. By assuming the isotope shift to be negligible the authors could determine the most probable value of the nuclear spin of Kr^{83} to be $I = 9/2$.

The determination of such high spin values is always rather uncertain when based upon the Landé interval rule; this is especially the case, when deviations from this rule occur, caused by an electric quadrupole moment, which in the following years was found to exist for a number of nuclei. For these reasons H. KORSCHING[3] preferred to measure the relative intensities of the hfs components; his results, however, were found to con-

firm the spin value given by Kopfermann. Furthermore, Korsching measured deviations from the interval rule for one level and calculated thereby the quadrupole moment of Kr^{83} to be $Q = +0.15 \times 10^{-24}$ cm^2.

The smallness of the splittings in the hfs of the krypton lines and the unfavourable isotopic composition with respect to Kr^{83} in natural krypton makes investigations with separated isotopes most desirable. Such investigations have been made possible by the development of isotope separators during and after World War II. The commencement of spectroscopic work with separated isotopes of the noble gases was brought about in 1949 by means of an electromagnetic isotope separator built by J. Koch[4] at the Institute of Theoretical Physics in Copenhagen, where use was made of a new technique, designed by J. Koch[5], for collecting gaseous ions. This technique is based upon the fact, that when gaseous ions are accelerated by a voltage of about 50 kV and allowed to hit an aluminium target, they will penetrate the surface of the target to a certain depth, from which they can only be released by heating. Some preliminary results have been published on the isotopes of neon, krypton and xenon[6], and a more exhaustive publication has been given on the odd xenon isotopes[7]. The present paper contains results concerning even as well as odd isotopes of krypton.

2. Experimental Procedure.

The arc spectrum of krypton was excited in an ordinary discharge tube, which was made of pyrex glass and given the shape shown in fig. 1. The capillary bore was 1 mm and the total volume of the tube was 25 cm^3. The cylindrical electrodes consisted of aluminium plates $2\frac{1}{2} \times 4$ cm wrapped around themselves; one of these, T, had previously been irradiated in the isotope separator with ions of the isotope in question.

The procedure in preparing the tube was the following: First a helium tube of the shape mentioned, in which two non-irradiated aluminium electrodes were mounted, was manufactured in the usual way, i. e. the glass walls were degassed by heating with a flame and both electrodes were degassed thoroughly by repeated

heating with the aid of a high-frequency coil, which induced currents in the aluminium. The tube was then filled with helium to a pressure of a few mm of *Hg* and sealed off. To make sure that no leaks existed, it was ascertained that the tube still emitted a pure helium spectrum after having stood for a day or two. The tube was then re-opened and the horizontal electrode was replaced by the target plate *T*, containing the isotope in question.

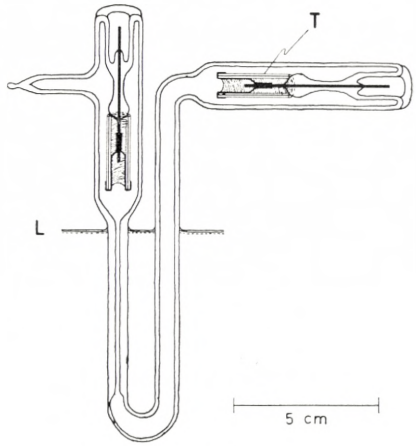

Fig. 1.

Helium was inserted for the second time and after sealing off the spectrum emitted was again seen to be purely helium. Finally, the target electrode was heated by induction currents in order to release the krypton gas collected in it. Helium now acts as a carrier gas enabling the tube to emit a fairly strong krypton spectrum, in spite of the small amounts (50 to 100 micrograms) of krypton available. In order to avoid impurities the target plate was handled exclusively by cleansed tools, and furthermore, the target plate had been degassed thoroughly before it was used as a collector.

The pressure of helium was chosen at 7 mm *Hg*, which was found to give the optimum excitation conditions. The tube was fed with an a.c. from a 7000 volt transformer, connected in series with a balance resistance of 300 000 ohm to enable the tube to be run at a low current (approx. 5 mA) in order to get as sharp lines as possible. The Doppler broadening was

further diminished by inserting the tube in an unsilvered Dewar vessel containing liquid air to the level L indicated in fig. 1.

The spectroscopic equipment consisted of a Steinheil 3-prism glass spectrograph with focal lengths of 650 and 640 mm for the collimator and the camera respectively, and a Fabry-Perot étalon with 60 mm plates, placed in the parallel beam of light between collimator and prism. By means of an achromatic lens with $f = 195$ mm a double-sized image of the capillary tube was projected onto the slit. This illuminating lens, having a diameter of 60 mm, was able to produce full illumination throughout the whole length of the spectral lines.

Special care was taken in adjusting the Fabry-Perot étalons, whose construction allowed the existence of optical contact between the quartz plates and the invar spacer to be verified by the observation of Newton's rings. The final adjustment was carried out with the light from a low pressure mercury lamp and making use of a low power telescope (10×80), whose large exit pupil (8 mm) made it possible to observe the interference rings, even when the eye was moved into different positions. The following spacers were used: 12.5 — 15 — 25 — 35 — 50 mm, and the exact thicknesses were measured to an accuracy of 10^{-5} mm by means of spectral lines of interferometrically known wavelengths.

The strong infra-red krypton lines were photographed on Kodak IRER and Eastman IN emulsions and the visible lines on ordinary Kodak, Ilford or Agfa plates. The plates were measured with a Zeiss comparator, and the line separations were evaluated by the standard method of quadratic interpolation. For clearly separated lines an accuracy of about 0.2×10^{-3} cm^{-1} was obtained.

3. Isotope Shifts between the Even Isotopes*.

In the case of elements containing their natural mixture of isotopes the small isotope shifts of spectral lines can only be observed and measured down to a certain lower limit. This

* A short communication of these results was given at the Rydberg Centennial Conference in Lund in July 1954.

limit is set partly by the resolving power of the spectrographic equipment and partly by the finite line width due to the light source, and is usually of the order of magnitude 0.01 to 0.02 cm^{-1}, depending on the wavelength region. For krypton the isotope shifts are below this limit and can therefore not be observed by using unseparated krypton.

By using separated isotopes, however, it is possible to detect and measure still smaller shifts, far beyond the limit set by the resolving power. This is due to the well known fact, that the uncertainty involved in the measurement of the centre of gravity of a line is some ten times smaller than the half intensity width of the line itself.

Among the even krypton isotopes only 82, 84 and 86 are abundant enough to allow one to collect a sufficient amount within a reasonable time, and the present investigation is therefore confined to these three isotopes. Spectral tubes were made containing Kr^{82}, Kr^{84} and Kr^{86}, respectively, and the tubes were filled with helium to approximately the same pressure ($\pm$ 1 mm *Hg*) in order to avoid relative displacements effectuated by pressure differences.* By means of these tubes interferometer spectrograms were made, with spacers from 25 to 50 mm, using the following method of alternating exposures: First an exposure of, say, Kr^{84} was made; then the plate holder was displaced vertically and an exposure of Kr^{82} was made on a new area of the same plate; finally Kr^{84} was exposed again after a renewed displacement of the photographic plate. This method allows one to control the constancy of the optical device from the beginning to the end of the exposures. Only photographs showing a sufficient constancy were used for measurements. During longer exposures the étalon was placed in an air-tight box (supplied with plane windows) in an effort to counteract the effect of variations in the pressure and temperature of the surrounding air. For the stronger lines, which could be photographed in a few minutes, this precaution could often be avoided.

From such exposures the isotope shift is easily determined by measuring the diameters of the interference rings of both isotopes; the difference between these diameters then simply

* Unpublished work by V. Middelboe on Kr^{84} shows that the displacement caused by a helium pressure difference of 1 mm *Hg* is less than 0.0001 cm^{-1}.

corresponds to the shift between the isotopes. Both the shifts 82—84 and 84—86 were measured and found to be identical within the experimental error. Only the strongest krypton lines have been investigated, namely the $1s - 2p$ combinations (using the Paschen notation) in the infra-red and visible regions, and the $1s - 3p$ combinations in the blue part of the spectrum. The results are collected in table 1, which for each line contains the mean value of the measurements made on a large number of plates; the figures are expected to be accurate to within 10 %.

TABLE 1.

Wave-length Å	Transition	Shift cm^{-1}	Wave-length Å	Transition	Shift cm^{-1}
8928	$1s_5 - 2p_{10}$	2.8×10^{-3}	7685	$1s_2 - 2p_1$	4.4×10^{-3}
8776	$1s_4 - 2p_8$	3.7	7601	$1s_5 - 2p_6$	2.4
8508	$1s_2 - 2p_4$	4.1	7587	$1s_4 - 2p_5$	3.8
8298	$1s_4 - 2p_7$	3.5	5870	$1s_4 - 2p_2$	3.8
8281	$1s_2 - 2p_3$	4.4	5570	$1s_5 - 2p_3$	2.9
8263	$1s_2 - 2p_2$	4.4	4502	$1s_4 - 3p_8$	4.8
8190	$1s_4 - 2p_6$	3.4	4463	$1s_4 - 3p_7$	5.0
8112	$1s_5 - 2p_9$	2.2	4453	$1s_4 - 3p_6$	4.9
8104	$1s_5 - 2p_8$	2.5	4376	$1s_4 - 3p_5$	4.7
8059	$1s_3 - 2p_4$	2.6	4362	$1s_5 - 3p_{10}$	5.0
7854	$1s_3 - 2p_3$	2.8	4319	$1s_5 - 3p_9$	4.0
7694	$1s_5 - 2p_7$	3.5	4273	$1s_5 - 3p_6$	4.0

The sign of the observed shifts was in all cases such that the wavenumbers increased for increasing mass numbers, i. e. in the order 82—84—86, which is the order to be expected when dealing with a normal mass effect. The magnitude of the observed shifts also corresponds rather nearly to that to be expected from a mass effect.

As first recognized by N. BOHR the mass effect for light elements can be ascribed to the motion of the nucleus, the finite mass of which varies slightly from one isotope to another. According to Bohr's theory this gives rise, in the case of one-electron spectra, to a displacement ΔE of a level E given by the formula:

$$\Delta E = E \cdot \frac{M_2 - M_1}{M_1 \cdot M_2} \cdot m$$

where M_1 and M_2 are the masses of the two isotopes in question, and m the mass of the electron, which is $1/1836 = 5.49 \times 10^{-4}$ in chemical mass units. For krypton with $M_1 = 82$ and $M_2 = 84$ one gets

$$\Delta E = E \frac{2}{82 \times 84} 5.49 \times 10^{-4} = 1.6 \times 10^{-7} E.$$

By means of this formula the term displacements in table 2 have been calculated in units of 10^{-3} cm $^{-1}$. In atoms with more than one electron there is, in addition to this simple mass effect, a specific mass effect due to correlations in the motions of the electrons.

The final comparison between the measured line shifts and the calculated term displacements cannot be made until further measurements of higher series members have furnished absolute values for the term shifts. Certain information can be obtained, however, by making the rather crude assumption that the displacements for the higher terms ($2p$ and $3p$) are due mainly to the simple mass effect. Consequently, by adding the observed line shifts to the theoretical displacements for the $2p$ and $3p$ terms one can obtain empirical mean values for the $1s$ term displacements, which can then be compared with the theoretical ones. This has been done in table 2 under the columns ΔE_{calc} and ΔE_{obs}.

From these figures it may be stated that for $1s_5$ and $1s_3$ only small deviations occur, whereas for $1s_4$ and especially for $1s_2$ the simple mass effect alone cannot be responsible for the observed effect. In spite of the smallness of the observed shifts in krypton it is reasonable to conclude, that these shifts for the most part can be accounted for by Bohr's formula, and that only for the deepest term ($1s_2$) a specific mass effect, of the order of magnitude $+ 2 \times 10^{-3}$ cm^{-1}, can be established with certainty.

This result is in accordance with those found by R. Ritschl and H. Schober[8] in neon, where absolute values of term shifts were obtained, and by H. Kopfermann and H. Krüger[9] in

TABLE 2.

	E	ΔE_{cal}	ΔE_{obs}	$\Delta E_{obs} - \Delta E_{cal}$
$1s_5$	32943	5.3	5.8	0.5
$1s_4$	31998	5.1	6.5	1.4
$1s_3$	27723	4.4	5.1	0.7
$1s_2$	27068	4.3	6.7	2.4

		ΔE_{cal}			ΔE_{cal}
$2p_{10}$	21746	3.5	$3p_{10}$	10028	1.6
$2p_9$	20620	3.3	$3p_9$	9799	1.6
$2p_8$	20607	3.3	$3p_8$	9793	1.6
$2p_7$	19950	3.2	$3p_7$	9601	1.5
$2p_6$	19791	3.2	$3p_6$	9552	1.5
$2p_5$	18822	3.0	$3p_5$	9153	1.5
$2p_4$	15319	2.5			
$2p_3$	14996	2.4			
$2p_2$	14970	2.4			
$2p_1$	14060	2.2			

argon, where only relative shifts were measured; the latter results were confirmed later by HORST MEYER[10] using separated isotopes.

4. Hyperfine Structure and Term Intervals of Kr^{83}

The purpose of investigating the odd krypton isotope Kr^{83}, procured by the separation of natural krypton, was to obtain further evidence on the spin value, previously found, and to get an improved value for the electric quadrupole moment of this nucleus. Although the isotopic separation in the present case appeared to be not quite perfect, owing to the large initial abundance of the two neighbouring isotopes 82 and 84, the hfs components of all the observed lines were much better resolved than for natural krypton. The six lines listed in table 3 were selected for measurements, as these lines were by far the best resolved and were most easily analysed. Previous investigators, working with unseparated krypton, also used these lines.

TABLE 3.

Wave-length Å	Transition	Total splitting cm^{-1}	Spacer, max. mm.	Remarks
8508	$1s_2 - 2p_4$	0.245	15	Control of $1s_2$ and $2p_4$
8281	$1s_2 - 2p_3$	0.321	12.5	Control of $1s_2$ and $2p_3$
8059	$1s_3 - 2p_4$	0.192	15	Gives $2p_4$ splitting
7854	$1s_3 - 2p_3$	0.075	35	Gives $2p_3$ splitting
7685	$1s_2 - 2p_1$	0.246	15	Gives $1s_2$ splitting
5570	$1s_5 - 2p_3$	0.238	15	Gives $1s_5$ splitting

Each of these lines was measured on a large number of plates, and the greatest importance was attached to the choice of the largest étalon spacer that could be used in each particular case without the overlapping of neighbouring orders. The following diagrams, figs. 2—7, show the term transitions and below these

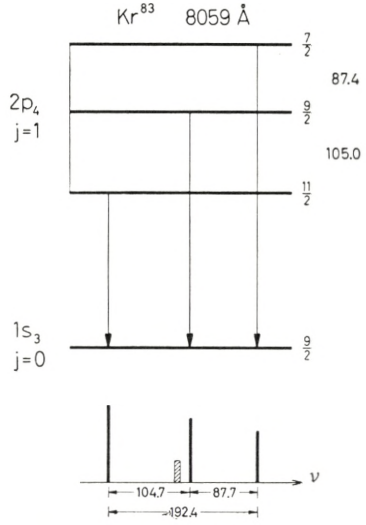

Fig. 2.

the line structures; beneath the latter the mean values of some of the measured intervals are given in units of 10^{-3} cm $^{-1}$, while at the right of each term diagram the finally adopted term intervals are written in the same units. In each line picture the hfs

components are fully drawn and the component due to the even isotopes is shown hatched. The heights of the lines are drawn proportional to the calculated intensities. The reader can find the magnitude (in units of 10^{-3} cm $^{-1}$) of any required line interval, which is not already given, by measuring the particular distance

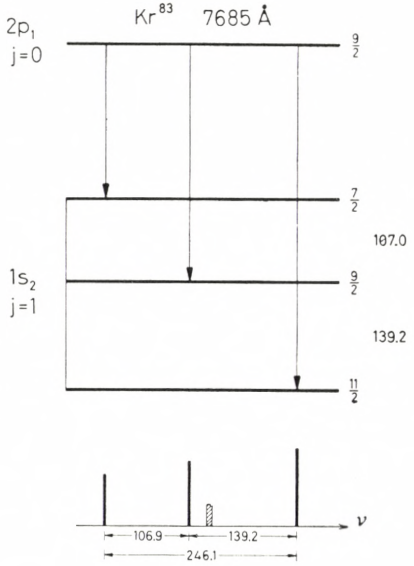

Fig. 3.

in the line picture to the nearest $^1/_{10}$ mm and multiplying by 10. Further, it may be instructive to compare the diagrams fig. 2—7 with the corresponding enlarged photographs of the line structures printed on the special plate at the end of this paper.

In order to explain how the term splittings have been evaluated from the line structures, the individual lines will now be discussed in the proper logical order. For 8059 Å, $1s_3 - 2p_4$, fig. 2, the line structure should be identical with the splitting of $2p_4$, as $1s_3$ with $j = 0$ cannot split. However, only the total splitting can be measured with certainty, because the distance between the component (hatched) coming from the even isotopes and the central hfs component is only about 0.016 cm^{-1}, and this gives rise to an attraction of the central component and thereby a distortion of the intervals.

In order to overcome this difficulty the lines 7685 and 8508 were used as auxiliary lines. For 7685 Å, $1s_2 - 2p_1$, fig. 3, the upper term $2p_1$ cannot split, and the line structure therefore gives the splitting of $1s_2$. Here the disturbance of the intervals

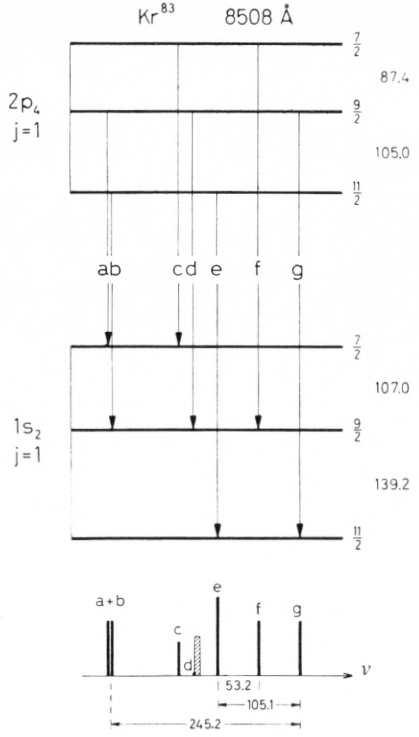

Fig. 4.

is considerably less than for 8059, as the separation of the hatched component and the central hfs component is more favourable, the distance between them being about 0.027 cm^{-1}.

The third line 8508 Å, $1s_2 - 2p_4$, fig. 4, is a combination between the two terms, which have just been discussed, and the measured intervals of this line can therefore give improved values for the splittings of both these terms. For instance the distance e—g gives the larger interval of $2p_4$, and the distance e—f subtracted from the total splitting of $2p_4$ gives the larger interval of $1s_2$. By means of the three lines discussed so far the splittings of the terms $1s_2$ and $2p_4$ can be found without any

one-sided disturbances and with an accuracy of about $\pm 0.2 \times 10^{-3}$ cm^{-1}.

A method similar to the one discussed above was used to determine the splitting of $2p_3$. For the line 7854 Å, $1s_3 - 2p_3$, fig. 5, only the total splitting is reliable, but the line 8281 Å, $1s_2 - 2p_3$, fig. 6, yields the intervals of $2p_3$ undisturbed by the

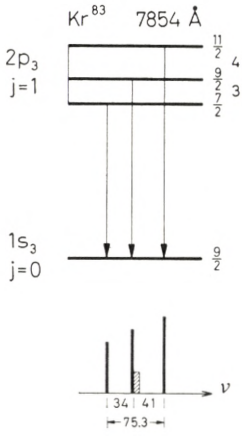

Fig. 5.

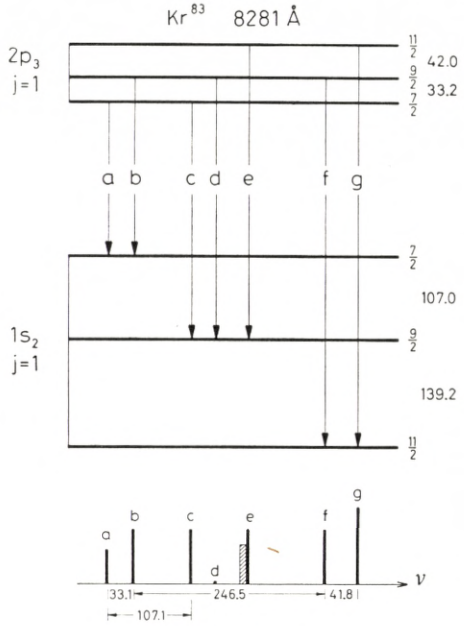

Fig. 6.

hatched component, namely as the distances *a*—*b* and *f*—*g*. Furthermore, the distances *a*—*c* and *b*—*f*, fig. 6, are equal to the smaller interval and the total splitting of $1s_2$, respectively, and this gives a final check on the hitherto measured intervals.

The two intervals of $2p_3$ then being established with some certainty, the next problem was to find the intervals of the term $1s_5$ by means of the line 5570 Å, $1s_5 - 2p_3$, fig. 7. For this particular line the great improvement achieved by the use of separated isotopes is most clearly demonstrated by the fact, that it was possible to distinguish seven separate components. In fig. 7 it will be seen, that the first (largest) interval of $1s_5$ is equal to the distance *h*—*i*, and that the second interval can be found by means

of the distance e—h, when the larger interval of $2p_3$ is known. The third interval of $1s_5$ is equal to the distance d—e and is found, as it happens, to coincide with the smaller interval of $2p_3$. Finally, the fourth and smallest interval of $1s_5$, namely a—b, is so small that a considerable mutual attraction of a and b is believed to take place, with the consequence that the directly measured value

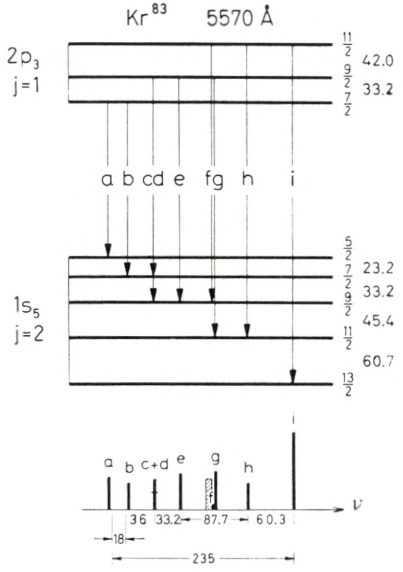

Fig. 7.

(0.018 cm^{-1}) for the distance a—b is too small. The magnitude of the mutual attraction could, however, be evaluated in the following way. The distance from the line $c + d$ to the displaced position of b was found by measurement to be 0.036 cm^{-1}; the true distance between these two lines is seen by consulting the term diagram to be 0.033 cm^{-1}; consequently, the amount by which b has been displaced towards a equals 0.003 cm^{-1}. The corresponding displacement of a towards b can then be calculated to be 0.002 cm^{-1}. This value was obtained by assuming the line shape to be Gaussian, i. e. mainly due to Doppler-broadening, and by taking the intensity ratio of a and b into account. In this way a total mutual attraction of 0.005 cm^{-1} is found, which, when added to the directly measured distance

from a to b, gives the corrected value 0.023 cm^{-1} for the smallest interval of $1s_5$. The finally adopted intervals for $1s_5$, written in fig. 7, will be discussed later.

5. Nuclear Moments of Kr^{83}.

It appears from the fine structure quantum numbers F, written opposite each term component in the figs. 2—7, that one has adopted the spin value $I = {}^9/_2$. If one tries to confirm this value by means of the Landé interval rule, one does not get a complete agreement for any of the observed terms. Table 4 shows the intervals calculated from the measured total splittings by the interval rule for $I = {}^9/_2$, together with the observed intervals. The deviations, which are large for $1s_2$ and $1s_5$ and rather

TABLE 4.

$1s_2$		$1s_5$		$2p_3$		$2p_4$	
obs.	calc.	obs.	calc.	obs.	calc.	obs.	calc.
139.2 ± 0.3	135.4	60.3 ± 0.5	53	42.0 ± 0.4	41.4	105.0 ± 0.2	105.8
107.0 ± 0.3	110.8	45.7 ± 0.5	45	33.2 ± 0.4	33.8	87.4 ± 0.2	86.6
246.2 ± 0.3	246.2	33.2 ± 0.5	36	75.2 ± 0.4	75.2	192.4 ± 0.2	192.4
		23 ± 1	28				
		162 ± 1	162				

small for $2p_3$ and $2p_4$, must in all cases be ascribed to the action of a quadrupole moment of the nucleus. Even the term $2p_4$, which in pure jj-couping should be expected to have a spherically symmetrical electric field in which the quadrupole moment of the nucleus should produce no effect, shows a deviation appreciably larger than the uncertainty of the measurements. The same is found to be the case on calculating the intervals for $I = {}^{11}/_2$; one then gets a deviation for $2p_4$, which is of the same size but of opposite sign.

This dilemma has recently been resolved by an investigation of the hyperfine structure of some krypton lines using the radioactive isotope Kr^{85}, produced by fission processes.[11] Having

two odd isotopes of the same element at ones disposal, i. e. two different nuclei with identical electron configurations, one must find that the ratio between the two deviations from the interval rule is constant from term to term, this constant simply being equal to the ratio between the quadrupole moments of the two nuclei. This was found to be the case only when assuming $I = {}^9/_2$ for both isotopes. The deviation found for $2p_4$ may then be explained as due to a lack of spherical symmetry for this term, owing to the intermediate coupling conditions in krypton.

As the spin value of Kr^{83} thus must be considered to be established with certainty, it is now possible to calculate the nuclear quadrupole moment from the observed intervals. The first step in this calculation will be to separate the magnetic and the electrostatic contributions to the hyperfine structure by evaluating the a- and b-factors by means of the general theory on the interaction between nuclei and electrons.[12)]

According to this theory, the hyperfine structure of a given level can be described by the formula

$$E_F = E_0 + a \cdot \frac{C}{2} + b \left[\frac{3/4\ C(C+1) - I(I+1)\, J(J+1)}{2\, I(2\,I-1)\, J(2\,J-1)} \right]$$

where

$$C = F(F+1) - J(J+1) - I(I+1).$$

E_0 is the energy of the undisplaced level, i. e. without any hyperfine structure, and E_F is the energy of the level component having the fine structure quantum number F. J is the inner quantum number of the level and I the nuclear spin. a and b are the magnetic and electric interval factors, respectively.

The evaluation of the a- and b-factors is simply carried out by the following scheme (table 5), in which the values of E_F are calculated for $I = {}^9/_2$ for the two cases $J = 1$ and $J = 2$. By subtracting adjacent term components E_F the term intervals ΔE, given in the last column, are found. It will be seen from the expressions ΔE, that the Landé interval rule comes out, when $b = 0$, i. e. if no quadrupole moment is present.

By inserting the observed intervals from table 4 in the expressions ΔE one gets the equations, from which the numerical values of a and b can be found. For a term with $J = 1$ ($1s_2$,

TABLE 5.

J	F	C	E_F	ΔE
	11/2	9	$E_{11/2} = E_0 + \frac{9}{2}a + \frac{1}{4}b$	$E_{11/2} - E_{9/2} = \frac{11}{2}a + \frac{11}{12}b$
1	9/2	—2	$E_{9/2} = E_0 - a - \frac{2}{3}b$	$E_{9/2} - E_{7/2} = \frac{9}{2}a - \frac{9}{8}b$
	7/2	—11	$E_{7/2} = E_0 - \frac{11}{2}a + \frac{11}{24}b$	
	13/2	18	$E_{13/2} = E_0 + 9a + \frac{1}{4}b$	$E_{13/2} - E_{11/2} = \frac{13}{2}a + \frac{13}{24}b$
	11/2	5	$E_{11/2} = E_0 + \frac{5}{2}a - \frac{7}{24}b$	$E_{11/2} - E_{9/2} = \frac{11}{2}a$
2	9/2	—6	$E_{9/2} = E_0 - 3a - \frac{7}{24}b$	$E_{9/2} - E_{7/2} = \frac{9}{2}a - \frac{5}{16}b$
	7/2	—15	$E_{7/2} = E_0 - \frac{15}{2}a + \frac{1}{48}b$	$E_{7/2} - E_{5/2} = \frac{7}{2}a - \frac{7}{16}b$
	5/2	—22	$E_{5/2} = E_0 - 11a + \frac{11}{24}b$	

$2p_3$ and $2p_4$) one gets just two equations for the determination of the two quantities a and b. For $1s_5$ with $J = 2$, however, four equations are obtained for the determination of a and b, so in this case a graphical method is preferred in order to obtain the most probable values. The four equations for $1s_5$

$$\text{I} \qquad \frac{13}{2}a + \frac{13}{24}b = 60.3$$

$$\text{II} \qquad \frac{11}{2}a = 45.7$$

$$\text{III} \qquad \frac{9}{2}a - \frac{5}{16}b = 33.2$$

$$\text{IV} \qquad \frac{7}{2}a - \frac{7}{16}b = 23$$

are plotted in the following diagram (fig. 8) as the straight lines I, II, III and IV, which should be expected to intersect in a

single point. This is the case within the accuracy of the measurements, as will be seen by the vertical short lines drawn at the left. These vertical lines indicate the parallel displacements of the four straight lines that correspond to the uncertainties of the

Graphical evaluation of the a- and b-factors

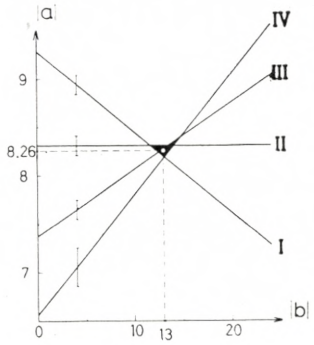

Fig. 8.

four intervals of $1s_5$. From the centre of intersection one gets $a = 8.26$ and $b = 13$.

By using the a- and b-factors, here determined, one can calculate the most reliable intervals for $1s_5$; these are given in fig. 7 and listed in table 6 together with the final results for the other three terms examined. The latter were chosen as making the best overall fit with the experimental results.

For the calculation of the quadrupole moment the term $1s_5$

TABLE 6.

Term	J	F	Intervals	a	b
$1s_2$	1	$\frac{11}{2}\ \frac{9}{2}\ \frac{7}{2}$	— 139.2, — 107.0	— 24.70 ± 0.06	— 3.7 ± 0.4
$1s_5$	2	$\frac{13}{2}\ \frac{11}{2}\ \frac{9}{2}\ \frac{7}{2}\ \frac{5}{2}$	— 60.7, — 45.4, — 33.2, — 23.2	— 8.26 ± 0.08	—13 ± 1
$2p_3$	1	$\frac{11}{2}\ \frac{9}{2}\ \frac{7}{2}$	+ 42.0, + 33.2	+ 7.54 ± 0.08	+ 0.6 ± 0.5
$2p_4$	1	$\frac{11}{2}\ \frac{9}{2}\ \frac{7}{2}$	— 105.0, — 87.4	— 19.23 ± 0.04	+ 0.8 ± 0.3

must be preferred. This term has not only the largest b-factor, but further, quite analogous to xenon,[7] the calculation for this term can be carried out independently of the type of coupling. According to the theory for the quadrupole interaction, the quadrupole moment Q can be found by the expression

$$-Q \cdot \overline{(3\cos^2\theta - 1)} \cdot \overline{\left(\frac{a_0}{r}\right)^3} \cdot 7.89 \cdot 10^{-3} = b \cdot 10^{-24}$$

where $\overline{(3\ cos^2\ \theta - 1)}$ is a measure for the deviation from spherical symmetry of the charge density of the electrons for the electronic state in question and for $1s_5$ will have the value $+ {}^2/_5$. The quantity $\overline{\left(\frac{a_0}{r}\right)^3}$, where a_0 is the radius of the first hydrogen orbit and r the distance of the electron from the centre of the nucleus, can be calculated by the following expression

$$\overline{\left(\frac{a_0}{r}\right)^3} = 0.114 \cdot \Delta \cdot \frac{R'}{Z_i \cdot H}$$

where Δ is the doublet separation of the ground state of the ion, Z_i the effective nuclear charge, and R' and H are relativistic correction factors. With the following numerical values $\Delta = 5220\ \text{cm}^{-1}$, $Z_i = 36 - 4 = 32$, $H = 1.03$ and $R' = 1.045$ one obtains $\overline{\left(\frac{a_0}{r}\right)^3} = 18.9$.

By inserting these quantities in the expression for Q one gets

$$\underline{Q = +(0.22 \pm 0.02) \times 10^{-24}\,\text{cm}^2.}$$

The term $1s_2$, used by KORSCHING[3], is not as well suited as $1s_5$ for the calculation of Q. A comparison between the b-factors of these two terms may, however, be carried out by a consideration quite similar to that used in the case of xenon.[7]

For $1s_2$ the wave function can be written in the form

$$\psi = c_1 \cdot \varphi\left(\frac{3}{2}, \frac{1}{2}\right) + c_2 \cdot \varphi\left(\frac{1}{2}, \frac{1}{2}\right)$$

where the coefficients c_1 and c_2 can be determined from the multiplet structure (i. e. from the relative positions of $1s_2$, $1s_3$, $1s_4$ and $1s_5$) as well as from the Zeeman effect. Both determinations yield $c_1 = 0.156$ and $c_2 = -0.988$. The b-factor of $1s_2$ can then be calculated from the b-factor of the ion ($P_{3/2}$) by the formula

$$b\ (1s_2) = \frac{1}{2} \cdot b\ (P_{3/2}) \left(c_1^2 - \frac{4}{\sqrt{2}} \cdot \frac{S}{R'} \cdot c_1 \cdot c_2 \right)$$

where $R' = 1.045$, $S = 1.07$, and $b\ (P_{3/2}) = b\ (1s_5) = (13 \pm 1) \times 10^{-3}\ \mathrm{cm}^{-1}$. One then gets

$$b\,(1s_2) = \frac{1}{2}\, b\,(1s_5)\,(c_1^2 - 2.89 \cdot c_1\, c_2) = (3.1 \pm 0.3) \times 10^{-3}\ \mathrm{cm}^{-1}$$

to be compared with the observed value $(3.7 \pm 0.4) \times 10^{-3}\ \mathrm{cm}^{-1}$.

The authors wish to thank Professor Niels Bohr for kindly placing spectroscopic equipment at their disposal and Dr. Aage Bohr for valuable theoretical discussions. We are further very grateful to Dr. J. Koch and Mr. K. O. Nielsen, C. E. for the most thorough isotope separations and to Mr. P. W. Streander for the careful construction of apparatus. Finally, we are indebted to the *Carlsbergfond* and to *Statens almindelige Videnskabsfond* for grants given to this work.

Physics Department.
Royal Veterinary and Agricultural College
Copenhagen, Denmark.

References.

1) C. J. Humphreys: Bur. Stand. Jour. Res. **7**, 453, 1931.
2) H. Kopfermann and N. Wieth-Knudsen: Zs. f. Phys. **85**, 353, 1933.
3) H. Korsching: Zs. f. Phys. **109**, 349, 1938.
4) J. Koch and B. Bendt-Nielsen: Dan. Mat. Fys. Medd. **21**, No. 8, 1944.
5) J. Koch: Nature **161**, 566, 1948.
6) J. Koch and E. Rasmussen: Phys. Rev. **76**, 1417, 1949, **77**, 722, 1950.
7) Aa. Bohr, J. Koch and E. Rasmussen: Ark. f. Fys. **4**, 455, 1952.
8) R. Ritschl and H. Schober: Phys. Zeitschr. **38**, 6, 1937.
9) H. Kopfermann and H. Kruger: Zs. f. Phys. **105**, 389, 1937.
10) Horst Meyer: Helv. Phys. Acta. **26**, 811, 1953.
11) E. Rasmussen and V. Middelboe: Zs. f. Phys. **141**, 160, 1955.
12) H. B. G. Casimir: Teylers Tweede Genootschap. Haarlem 1936.

Indleveret til selskabet den 7. juni 1955.
Færdig fra trykkeriet den 1. oktober 1955.

Fig 2 a. 8059 Å

Fig. 3 a. 7685 Å

Fig. 4 a. 8508 Å

Fig. 5 a. 7854 Å

Fig. 6 a. 8281 Å

Fig. 7 a. 5570 Å

Photographs of single orders of Kr-83 lines, enlarged 10–20 times. The direction of increasing wave numbers is from left to right, as in the corresponding diagrams figs. 2–7, but in the photographs the scale is of course not linear.